Analyst

Interdisciplinary detection science

www.rsc.org/analyst

Volume 137 | Number 4 | 21 February 2012 | Pages 789–1040

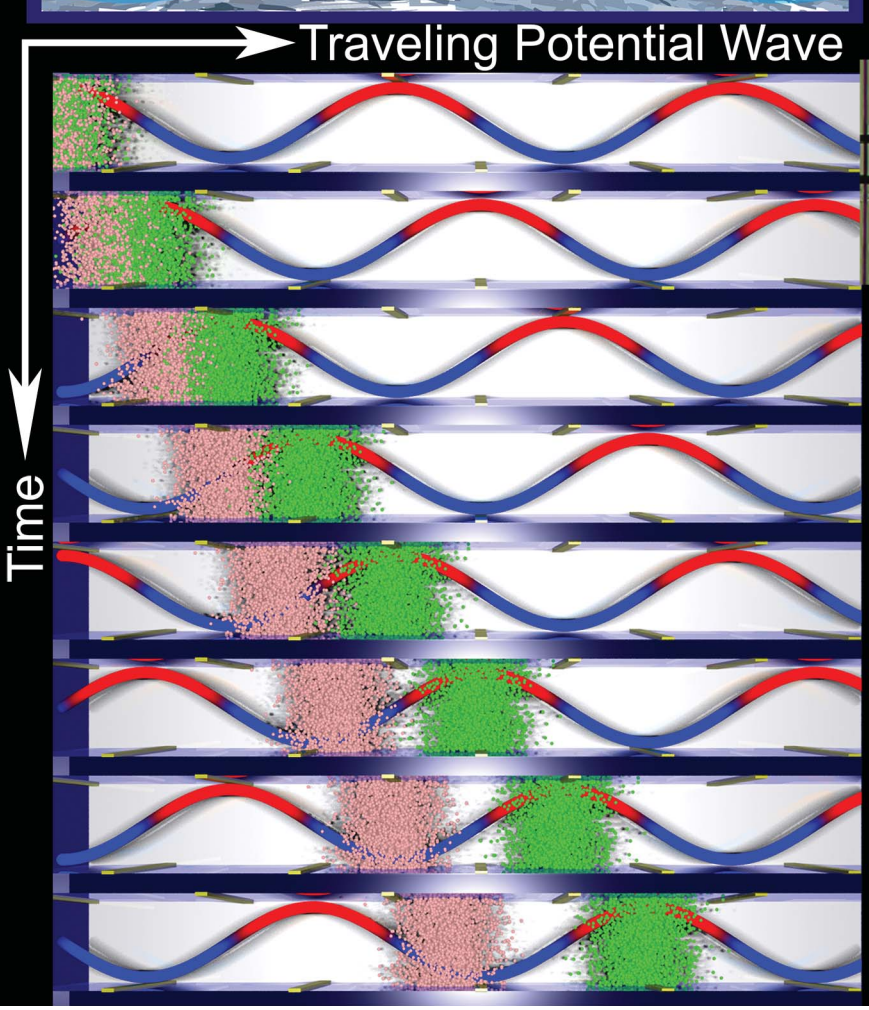

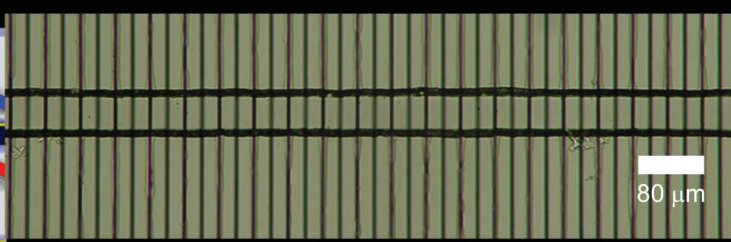

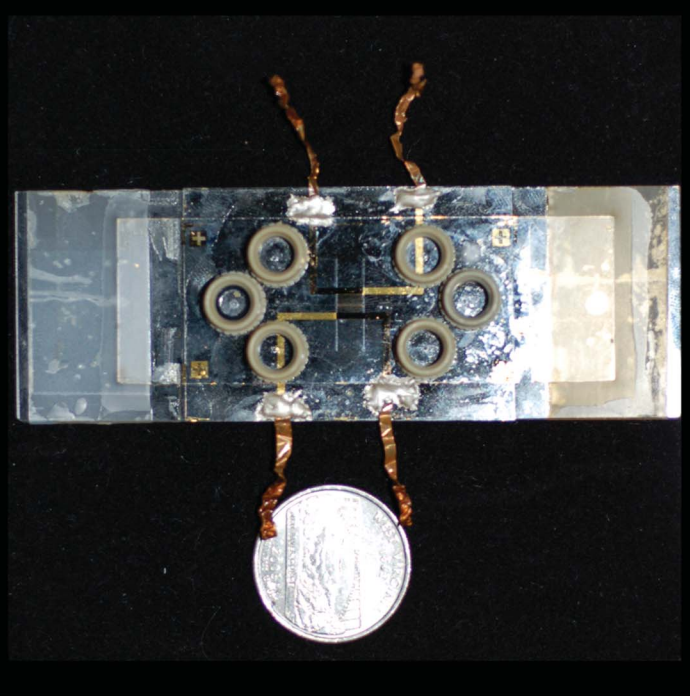

ISSN 0003-2654

RSC Publishing

PAPER

Aaron T. Timperman *et al*.

Fabrication and performance of a microfluidic traveling-wave electrophoresis system

0003-2654(2012)137:4;1-H

Analyst

Dynamic Article Links

Cite this: *Analyst*, 2012, **137**, 875

www.rsc.org/analyst

PAPER

Fabrication and performance of a microfluidic traveling-wave electrophoresis system†

Kyoo D. Jo, Jarrod E. Schiffbauer, Boyd E. Edwards,‡ R. Lloyd Carroll and Aaron T. Timperman§

Received 30th July 2011, Accepted 30th October 2011
DOI: 10.1039/c1an15669a

A microfluidic traveling-wave electrophoresis (TWE) system is reported that uses a locally defined traveling electric field wave within a microfluidic channel to achieve band transport and separation. Low voltages, over a range of −0.5 to +0.5 V, are used to avoid electrolysis and other detrimental redox reactions while the short distance between electrodes, ~25 μm, provides high electric fields of ~200 V cm^{-1}. It is expected that the low voltage requirements will simplify the future development of smaller portable devices. The TWE device uses four interdigitated electrode arrays: one interdigitated electrode array pair is on the top of the microchannel and the other interdigitated electrode array pair is on the microchannel bottom. The top and bottom substrates are joined by a PDMS spacer that has a nominal height of 15 μm. A pinched injection scheme is used to define a narrow sample band within an injection cross either electrokinetically or hydrodynamically. Separation of two dyes, fluorescein and FLCA, with baseline resolution is achieved in less than 3 min and separation of two proteins, insulin and casein is demonstrated. Investigation of band broadening with fluorescein reveals that sample band widths equivalent to the diffusion limit can be achieved within the microfluidic channel, yielding highly efficient separations. This low level of band broadening can be achieved with capillary electrophoresis, but is not routinely observed in microchannel electrophoresis. Sample enrichment can be achieved very easily with TWE using a device with converging electric field waves controlled by two sets of independently controlled interdigitated electrodes arrays positioned serially along the microchannel. Sample enrichment of 40-fold is achieved without heterogeneous buffer/solvent systems, sorptive, or permselective materials. While there is much room for improvement in device fabrication, and many capabilities are yet to be demonstrated, it is anticipated that the capabilities and performance demonstrated herein will enable new lab-on-a-chip processes and systems.

Introduction

High performance liquid chromatography (HPLC) and capillary electrophoresis (CE) are commonly used for liquid-phase analytical separations. HPLC is known for its high degree of selectivity, achieved by altering the mobile and stationary phases. However, in HPLC, stationary phase mass transfer and mobile phase mass transport contribute to band broadening and reduce the maximum achievable separation efficiency. Such processes have been described using rate theory.[1] In addition to the ability of CE to perform very fast separations, CE provides the narrowest peaks and unrivaled separation efficiencies. Of CE methods, free zone capillary electrophoresis produces the highest separation efficiencies. In a properly controlled CE separation, molecular diffusion is the main cause of band broadening, and the high separation efficiencies can approach the diffusion-limit.[2,3] Another important characteristic is the control and flexibility of the separation when coupling it with detectors that provide structural information. For example, real-time control of the rate of sample injection into a MS would be a significant advantage, and flow modulation in HPLC and field modulation in CE methods have been developed for this purpose.[4–6] However, these methods increase band dispersion and thereby degrade the separation efficiency and peak capacity. Therefore, a method for flow modulation that did not adversely affect the separation efficient would be of great use.

There have been a few pioneering reports of TWE that have been demonstrated with single-sided devices. Lean *et al.* used a single-sided electrophoresis device to transport proteins in gels and presented a theoretical model.[7] The theoretical model for protein migration was validated by comparing the migration of proteins separated by two-dimensional gel electrophoresis (2DE) to the model. Their experimental results for the TWE device were

C. Eugene Bennett Department of Chemistry, West Virginia University, Morgantown, West Virginia, 26506

† Electronic supplementary information (ESI) available. See DOI: 10.1039/c1an15669a

‡ current address: Department of Physics, Utah State University, Logan, Utah 84321

§ current address: ERDC-CERL, Champaign, IL, 61822

limited to two images showing migration of a protein band. With the model, they distinguished synchronous and asynchronous transport, and the feasibility of a concentration mode. A related device was used to concentrate particles in free solution with a combined TWE and field flow fractionation (FFF) device.[8] The TWE-FFF device used 10-μm wide electrodes separated by 30-μm that were used to enrich 3-μm beads, 10-μm beads, and *B. thurengiensis*. In the current report, our TWE devices use much thinner electrodes that have a 2 μm width. Wei developed a numerical model for traveling-wave electrophoresis separations of colloids for systems whose wavelength is much greater than the channel width. However, the experimental design or fabrication of such a device was not reported.[9]

TWE distinguishes itself from other separation techniques by employing an electric field wave to transport charged species whose mobilities exceed a tunable threshold. Previously, we reported a 2D model of ion migration velocities in microfluidic TWE and found good agreement of the theoretical and experimental values.[10] The ion velocity can be either synchronous or asynchronous depending on the ratio of the ion's maximum allowable velocity (given by $v = \mu E$) to the wavespeed. The microfluidic TWE system has a sandwich or dual layer architecture in which there are interdigitated electrode arrays on both the top and bottom of the channel. An illustration that shows the basics of operation of TWE is presented in Fig. 1. A mixture of charged particles, with blue dots representing high mobility anions, red dots representing high mobility cations, and grey symbols representing uncharged and low mobility species, is represented at the left hand side of Fig. 1A. Each charged particle has an intrinsic electrophoretic mobility under an applied electric field that is proportional to the charge of the particle. A traveling-wave potential attracts all charged species, but since it moves down the channel, only those species with mobilities higher than the wave velocity are fully entrained by the wave and migrate at the wave speed. Because no species can move at a rate greater than allowed by its electrophoretic mobility, species with intermediate electrophoretic mobilities move forward a fraction of the time and backwards for a lesser fraction of the time, with the net velocity in the forward direction. Species whose mobility is much less than the wavespeed are stationary. To summarize, ion mobility can fall into three regimes: 1) the ions migrate at the wavespeed, 2) the ions migrate at a slower rate than the wavespeed, and 3) the ions are stationary at very high wavespeeds. This migration pattern makes it possible to modulate between separative and non-separative transport by simply changing the wavespeed. This capability is currently unique to TWE.

This method provides very low band dispersion, because the species are trapped within potential wells of the electric field wave and are continually refocused as they move through the channel. In other words, the analyte ions are trapped between the crests of longitudinal electric field waves that travel along the separation channel. The low dispersion and the ability to change the analyte migration by simply changing the wavespeed may yield a flow modulation method with reduced dispersion, although this possibility has not been explored directly yet. This paper provides the first experimental results for TWE separations, band broadening, and sample enrichment. Moreover, the fabrication of a novel dual layer device and the sample injection schemes are both reported for the first time. Injection of narrow

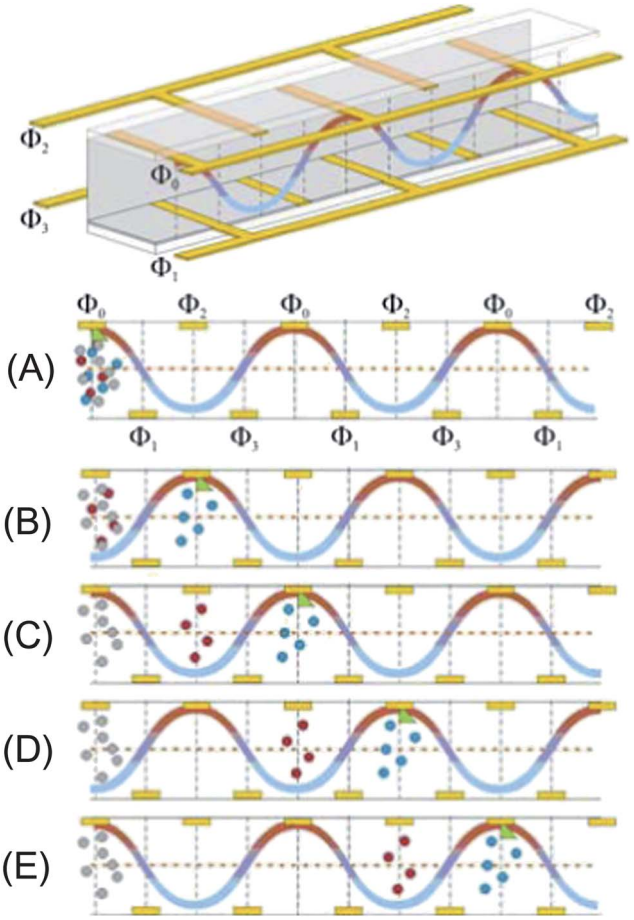

Fig. 1 At the top, an illustration of the four interdigitated electrode arrays that define the electric field within the microchannel are shown. The potential at each electrode, represented by Φ_0, Φ_1, Φ_2, Φ_3, is applied independently. Anions and cations are pushed in the same direction through the microchannel by the propagation of the electric field wave.

sample bands can be achieved with electrokinetic or hydrodynamic focusing of the sample in the injection cross, followed by application of the traveling electric field wave to move the focused band through the microchannel. Separation of a pair of standard dyes and proteins is demonstrated, and band broadening is measured at three different wavespeeds. The flexibility of the system is demonstrated with sample enrichment at the interface of two converging waves, providing a simple means of rapid sample enrichment. This method of sample enrichment is noteworthy because it requires no changes in buffer/solvents or the use of sorptive or permselective materials or structures that are difficult to fabricate. It is anticipated that the combination of low voltages and high separation efficiencies will make TWE separations well-suited for fieldable lab-on-a-chip (LOC) systems while the flexibility of the system will enable development of new microfluidic processing schemes.

Experimental

Chemicals and reagents

Unless otherwise noted all chemicals were purchased from Sigma-Aldrich (Milwaukee, WI). The running buffer was 10 μM

phosphate buffer, pH 7. The fluorescent dyes consisted of fluorescein and 6-[fluorescein-5(6)-carboxamido]hexanoic acid (FLCA) dissolved in running buffer. The protein mixture consisted of fluorescein isothiocyanate (FITC) labeled casein from bovine milk, and FITC labeled insulin from bovine pancreas.

Sylgard 184, a poly(dimethylsiloxane) prepolymer (PDMS) and curing agent, was from Dow Corning (Midland, MI). Tridecafluoro-1,1,2,2-tetrahydroctyl-1-trichlorosilane was from United Chemical Technologies (Bristol, PA). Distilled deionized water with a nominal resistivity of 18 MΩcm when dispensed from a Barnstead Nanopure Infinity system (Dubuque, IA) was used.

Device fabrication

Top and bottom electrodes were patterned on 25 × 75 mm, 1 mm thick glass slides (hereafter, thick glass slide)(Corning) and 35 × 50 mm, #1 cover glasses, nominally 0.13–0.16 mm thick (hereafter thin glass slide)(EMS Diasum) respectively, as described below. The thin glass slide facilitated optical microscopic observation of the sample plug inside the channel and enabled the fabrication approaches discussed later in this section. The thick glass slide for the top electrode substrate of the device provided structural stability for the device and was drilled with through-holes and fitted with reservoir attachments to provide inlet/outlet for sample and buffer solutions. The patterned electrodes are composed of interdigitated microelectrode arrays branched from each bus electrode (1 mm wide). The bus electrodes were used for electrical connections between the microelectrode arrays and an external signal generator. The width of each microelectrode was 2 μm with a pitch (distance between microelectrodes with the same potential) of 80 μm resulting in a fixed wavelength of 80 μm for the traveling-wave. Both sets of electrodes were defined using positive photolithography and development. A 20 nm titanium adhesion layer and 120 nm of gold were deposited on the patterned photoresist by e-beam evaporation (Temescal, Livermore, CA). After deposition of both metals, the substrates were sonicated in acetone to dissolve remaining photoresist and remove metal atop the photoresist layer. A schematic side view of a short section (equal to two wavelengths) of the four-electrode pattern is shown in Fig. 1. A device with a short separation channel equal to 4 mm or 50 wavelengths was used for the protein separation. For the other experiments, a device with longer 30 mm or 375 wavelength separation channel was used.

A microfluidic channel master was defined using SU-8 2010 negative photoresist (Microchem Corp, Newton, MA) on a silicon wafer (Silicon Sense, Nashua, NH) using conventional photolithography as shown in Figure S1.[11] Spin-coating conditions were optimized to produce a layer of SU-8 of 15 μm thickness on the wafer. An optical mask with 50 μm wide features was used to define the microfluidic channels in the SU-8 photoresist. After development of the SU-8 features, the master was silanized with tridecafluoro-1,1,2,2-tetrahydroctyl-1-trichlorosilane under vacuum for 1 h, then baked at 120 °C for 20 min to minimize adhesion of PDMS in the later molding steps. A 10 : 1 mixture of PDMS prepolymer and curing agent was mixed thoroughly and degassed under vacuum until all air bubbles were removed. Microfluidic channels were patterned in PDMS attached to the gold patterned thin glass slide electrode using a mold-cure-release method (Figure S1). The uncured PDMS mixture was applied in a thin coat to the channel master and the thin glass slide was placed onto the channel master with the electrode side facing the master. Using a Leica GZ 6 stereo microscope (Wetzlar, Germany), the microelectrode array was aligned with the microfluidic channels defined by SU-8 2010 such that microelectrode arrays at the sample inlet side cover the injection tee, and the separation channel was at right angles to the microelectrode arrays. Alignment marks at the corners of the electrode pattern and the microfluidic pattern facilitated alignment. A sheet of ACLAR® film (polychlorotrifluoroethylene, PCTFE, SPI Supplies, Westchester, PA) was placed on the thin glass slide aligned with the channel master and 500 grams of weight was used to press the thin glass slide into maximum contact with the SU-8 master, to define the microfluidic channels in a thin layer of PDMS. The PDMS was cured at room temperature for 24 h. The PDMS-embossed thin glass slide was released from the channel master by brief immersion in acetone. The flexibility of the thin glass slide facilitated release from the master. Acetone caused the reversible swelling of the cured PDMS,[12] inducing release from the master without deformation of the channel. The cured PDMS on the thin glass slide was rinsed with isopropanol and blown dry with nitrogen gas.

Six access holes for microfluidic coupling were drilled through the thick glass slide using a microdrilling station (Model 7000 Drill Press, Servo Products Company, Pasadena, CA) with a stereomicroscope for visualization. 1.01 mm ID drill bits from Kyocera Tycom Corporation (Irvine, CA) were used for drilling the access holes. The thick glass slide with access holes was sonicated in water for 2 min, rinsed with isopropanol and blown dry with nitrogen gas. Conductive silver paint (GC Electronics, Rockford, IL) was diluted 1 : 1 with acetone and applied to extend the bus electrodes over the edge of the thick glass slide for later electrical connection to the external signal generator. The electrodes on the thick glass slide were coated with a thin layer of PDMS to minimize deleterious electrochemical processes that might occur during the electrokinetic injection and TWE process. The thick glass slide was spin-coated with thinned PDMS solution (10% w/w of PDMS, including curing agent, in triethylamine) at 5000 rpm for 30 s, followed by baking at 120 °C for 20 min.

The top and bottom pieces were exposed to an air plasma in an RF-plasma cleaner (PDC-32G, Harrick Scientific, Ossining, NY) at 100 W for 12 s, then the two pieces were aligned and permanently bonded together such that the electrode arrays on top and bottom pieces were equally spaced (20 μm, Figure S2b). The alignment process was done manually on a homemade x-y-z translational stage combined with a rotational bottom stage under the stereomicroscope. The thick glass slide was held to the x-y-z stage by a see-through vacuum chuck, with the electrode array facing the thin glass slide attached to the rotational bottom stage. The two slide substrates were brought into near contact to visualize the electrode arrays in the same focal plane. The x-y position of the top slide and the rotation of the bottom slide were adjusted until the electrode arrays on top and bottom slides were equally spaced and parallel, then the two substrates were brought into contact for permanent bonding. After the alignment and contact process was completed, the vacuum was released and the

aligned device placed in an oven at 100 °C overnight with 500g of weight placed on top to press the slides together. The bus electrodes were connected to the external signal generator with copper tape (Ted Pella, Inc., Redding CA), silver paint, and silver epoxy (M.E. Taylor Engineering Inc., Rockville, MD). The bus electrodes on the PDMS-embossed thin glass slide were cleaned of residual PDMS with triethylamine and the silver paint was applied. Copper tape was attached on top of the silver paint and another layer of silver paint was applied on top of the tape. After the paint dried, the copper tape-electrode connection was reinforced by a thick layer of silver epoxy. The same process was used for attaching and fixing copper tape to the bus electrodes on the thick glass slide using the silver paint that was previously applied to the sides of the thick glass slide. Finally, six reservoirs (Nanoport, Upchurch Scientific, Oak Harbor, WA) were attached at the drilled access holes. This device features sets of interdigitated electrodes adhered to the top and bottom surfaces of a microfluidic channel defined in polydimethylsiloxane.

Device operation

In Fig. 1, a schematic view of a traveling-wave electrophoresis channel of height $h = 15$ μm formed by a lithographically-defined PDMS channel (grey) and two glass plates is shown. Interdigitated arrays of gold electrodes on the bottom surface of the top plate are held at oscillating electrical potentials $\Phi_0(t)$ and $\Phi_2(t)$. Similar arrays atop the bottom plate are held at potentials $\Phi_1(t)$ and $\Phi_3(t)$. In the diagrams, the initial wave direction is to the right. The potentials applied to the four electrodes are synchronized so that there is a 90° phase shift between adjacent electrodes, producing a propagating wave that traps ions whose mobilities exceed a tunable threshold. Injection of a narrow sample band was achieved with both electrokinetic (EK) and hydrodynamic (HD) focusing processes. For EK focusing process, a voltage of 75 V was applied to the electrode in sample reservoir for 30 s while the electrode in sample waste reservoir was held at ground. A voltage of 60 V was applied to the electrodes in running buffer reservoirs for pinched focusing. After the 30 s of focusing process, the sample plug was introduced into the separation channel by TWE. During this injection process, voltages of 10 V, 10 V, and 25 V were applied to the electrodes at sample, sample waste, and running buffer reservoirs respectively for clearing sample and waste streams (Fig. 3A). For HD focusing process, a vacuum was applied to the sample waste reservoir. Once a focused stream was obtained in the intersection, the vacuum was released and immediately afterward the TWE voltages were turned on, and the voltages of 10 V, 10 V, and 25 V were applied at sample, sample waste, and running buffer reservoirs respectively for clearing sample and waste streams (Fig. 3B).

Fluorescence imaging and device set-up

The fluorescence of sample bands were imaged using a Nikon TE-2000U Eclipse (Melville, NY) inverted fluorescence microscope with 10 × (0.45NA) and 2 × (0.1NA) objectives and captured with a CCD camera (Model 650, Roper Scientific, Tucson, AZ) (Fig. 6A). The 10× objective was used for all of the experimental studies, except the 2× objective was used for the stopped flow experiments to measure band broadening from diffusion. Images were collected at sampling rates up to 5.0 Hz and processed with MetaMorph (v6.2r6) and ImageJ (v8.1). Five reservoirs and the microchannel were filled with 10 μM sodium phosphate running buffer and one reservoir with the sample of interest. The TWE channel was aligned with the microscope objective such that the TWE channel length was oriented with the horizontal axis of the microscope stage. Electrical contact was made between the bus electrodes and a signal generator (LabSmith Inc., Livermore, CA). A six-step periodic potential approximating a sinusoidal potential was applied to the bus electrodes $\Phi_0(t)$- $\Phi_3(t)$ with an amplitude of 0.5 V at a controllable frequency (0.02–3.0 Hz). The following voltages were applied for the six step potential: 0.25, 0.5, 0.25, −0.25, −0.5, and −0.25 V. The first microelectrode at the injection tee is on the thin glass slide, and the second microelectrode is on the top thick glass slide, and so on.

Experimental determination of band broadening at the diffusion limit

The diffusion-limited band broadening was determined by measuring the increase in width of a fluorescein band in a TWE microchannel as a function of time in a stopped flow experiment. A narrow band of 15 μM fluorescein in 10 μM sodium phosphate was injected into the microchannel using hydrodynamic injection method. The sample band was brought into the region of interest (50 μm × 1659.809 μm) by TWE. The TWE was turned off and the dispersion of the band was imaged as a function of time. The intensity profiles of each time period were plotted as a function of distance. The 2× objective was used to visualize the entire length of the dispersing band in the channel. A 6-step periodic potential was applied with amplitude of 0.5 V.

Theoretical determination of band broadening at the diffusion limit

The theoretical calculations treated the plug in the channel as a 1D locally electro-neutral distribution of dye in aqueous buffer subject to possible external fields. In this case, the order of magnitude difference in buffer and analyte diffusivity can be shown to allow a further approximation wherein the buffer and analyte are effectively de-coupled to leading order with the buffer ions relaxing fast enough in comparison to the analyte. The time-evolution of an initial analyte distribution may be approximated by the Fourier transform solution of the single-species electro-neutral diffusion equation on an infinite domain as shown by the following equation:

$$n(x,t) = \frac{1}{2\sqrt{\pi D t}} \int_{-\infty}^{\infty} dx'\, n(x',0) \exp\left[-\frac{(x-x')^2}{4Dt} \right]$$

Here, n is the analyte concentration and D the analyte diffusivity, where the value 356 $\mu m^2\ s^{-1}$ is used. The initial analyte distribution $n'(x',0)$ is obtained from experimental data. Both the initial TWE and initial stopped-flow peaks were used as input and a theoretical value of the concentration profile for diffusion only is obtained by numerically evaluating the above equation at the desired times.

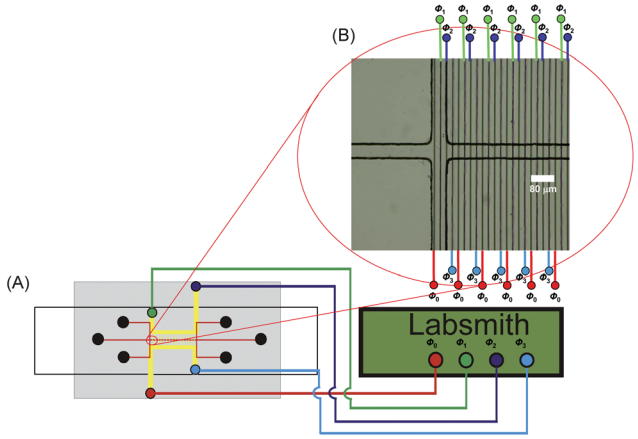

Fig. 2 **(a)** The connection of the signal generator to TWE microchip is illustrated. In the inset **(b)**, an optical micrograph of the injection tee is shown and the application of the different potentials is illustrated.

Sample enrichment

Sample enrichment experiments were carried out with the microchannel using a TWE device with two independently controlled sets of interdigitated electrode arrays with a total of eight applied potentials. The 15 nM fluorescein sample was injected continuously from one end of the device and transported toward the junction of the two TWE array sets at the device center. The voltage for each of the two TWE electrode array sets was programmed to generate converging potential waves that propagated toward the center of the device. A 6-step periodic potential was applied to each sets of the electrodes with amplitude of 0.5 V at 2.0 Hz. The increase in fluorescence intensity is measured as a function of time and compared with the intensity of standard fluorescein solutions in 10 μM sodium phosphate in the same channel with concentrations of 15, 150, 300, 450, and 600 nM.

Results and discussion

Fabrication

Fabrication of a two-layer TWE device is achieved using a PDMS spacer to define the microfluidic channel. The interdigitated electrode arrays are formed on the top and bottom slides of the device using lift-off, which provided well defined arrays of 2 μm wide electrodes. Alignment and proper spacing of the top and bottom electrode arrays is critical and we have found that good alignment, as shown in Fig. 2, can be achieved using a lab-built jig made with an x-y-z translational stage that holds the top slide and a rotating stage that holds the bottom slide. The pattern of the channel is molded into the uncured PDMS layer with a stamp made of SU-8 patterned with standard photolithographic techniques on a silicon wafer. The nominal height and width of the microchannel are 14 ± 1 μm and 55 ± 1 μm, respectively, and the walls are fairly straight and uniform as shown in Figure S2. The channel cross-section is trapezoidal in shape with the smaller more rounded segment at the top of microchannel. A residual PDMS film from the micromolding process covers the electrodes on the bottom substrate. To improve symmetry and increase the lifetime of the TWE electrode arrays, a nominally 100 nm thick film of PDMS is spun on the top substrate and its electrodes. The PDMS film thickness was measured to be 90–120 nm with atomic force microscopy of representative devices. The PDMS films prevent the solution from coming into direct contact with the electrodes, except for any imperfections that might exist. No imperfections could be

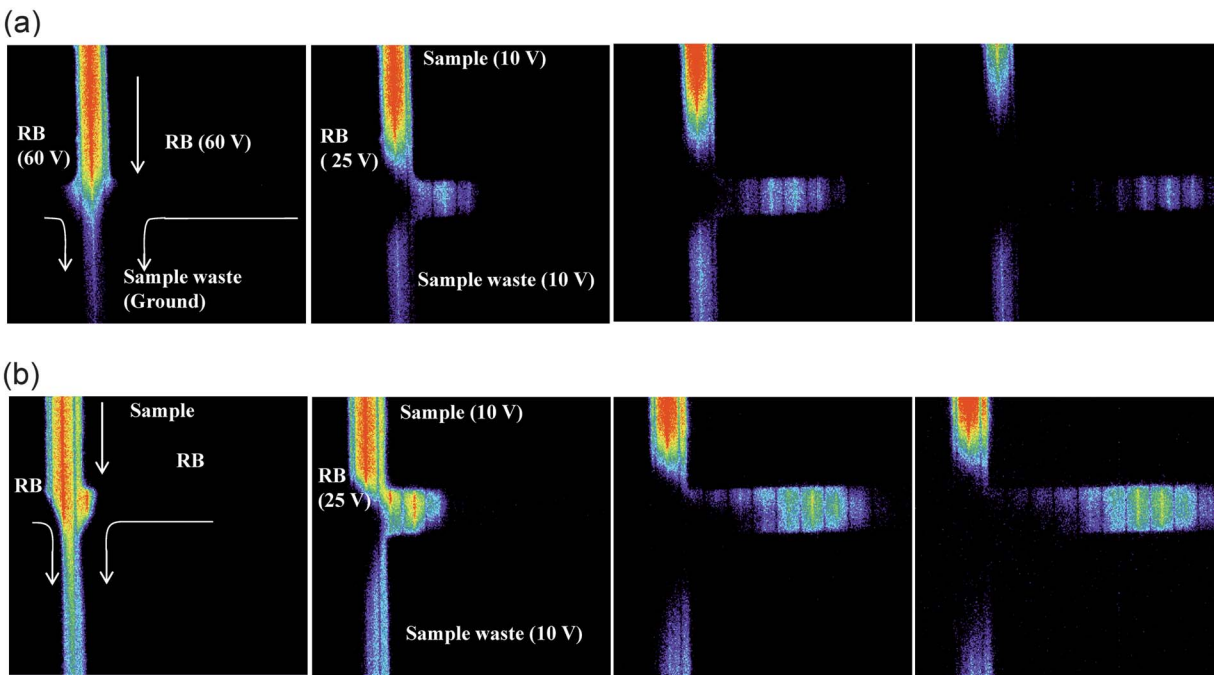

Fig. 3 Images of the electrokinetic (a) and hydrodynamic (b) injections of fluorescein are shown. To perform the injection into the horizontal TWE microchannel: the injection voltages or pressure is turned off as appropriate, voltages are applied for pull-back of the sample and waste streams, and the traveling wave potentials are applied to the TWE electrode array.

Table 1 Peak Dispersion

				Diffusion	
Wavespeed (Hz)	Initial $w_{1/2}$ (μm)	Elution Time (s)	TWE $w_{1/2}$ (μm)	Exper. $w_{1/2}$ (μm)	Theor. $w_{1/2}$ (μm)
1	963	206.71	1109	1246	1546
2	910	145.52	1173	1195	1324
3	909	119.52	1039	1124	1210
3	911	115.52	1042	1124	1210

observed with an optical microscope at 10X magnification for the devices used in this work. The maximum excursion of the potential, in excess of the +0.5 to −0.5 V used, is yet to be explored. Although the PDMS coatings covering the top and bottom substrates are not equivalent and the microchannel walls are neither vertical nor symmetric, the microchannel has proven to be sufficient for operation. It is anticipated that future improvements in device design and fabrication methods will provide improved performance.

Sample plug injection

An important step towards achieving a separation is injection of a relatively narrow sample plug. Ideally, the injected plug makes a negligible contribution to the width of the final plug. Both EK and HD sample plug injection methods have been developed, defining a narrow plug within the sample injection cross as shown by the optical micrographs in Fig. 3. The narrow plug is defined by pinching the band to be injected by flowing solution from the end of the separation channel and the running buffer reservoir at the sample injection cross, as indicated in Fig. 3A. In both the EK and HD pinched injections, the defined plug is moved out of the injection cross and through the microchannel by the simultaneous cessation of pinching flow and activation of the traveling electric field wave. The EK injection provides narrow injection plugs with an average plug width ($w_{1/2}$) of 172 μm and an RSD of 12%, although the EK injection profiles exhibit more tailing than the HD injections as shown in Table S1. The HD injections provided the most symmetric peaks, although the plug widths were much greater at 500 μm with a RSD of 8%. The greater width of the HD injection band is caused by broadening of the focused band that occurs as the vacuum is released.

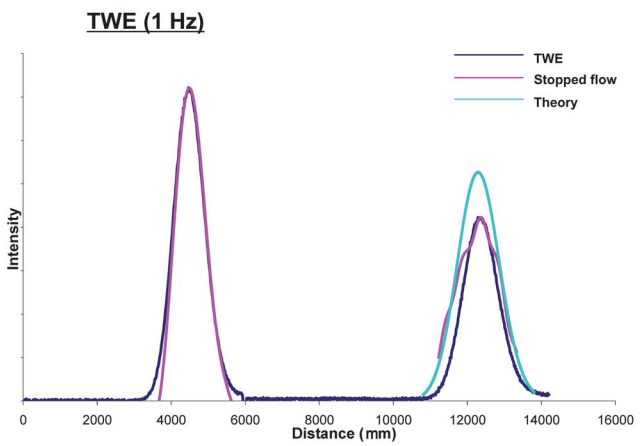

Fig. 4 A representative electropherogram from the band dispersion study that shows the initial and final band profiles for the transport of 15 μM fluorescein plug at 1 Hz. The experimental TWE data is compared with the experimental stopped flow data and the theoretical band dispersion by diffusion.

Sample migration

We have previously demonstrated that band migration could be achieved, and band velocity was reported as a function of wavespeed.[10] As anticipated, a neutral marker, riboflavin, did not migrate, indicating that electroosmotic flow (EOF) is negligible. An initial concern was the electrode charging caused by double layer formation would be so rapid that band migration could not be achieved. Mobility experiments with fluorescein plugs demonstrated that fluorescein migration could be achieved in 1μM but not 1 mM phosphate buffer (pH 7). A more extensive study of the concentration limit of background electrolyte and the analytes is yet to be performed. This requirement for low buffer concentration could be a serious limitation for applications if the sample solution is of higher ionic strength. However, there are also other applications, such as interfacing with ESI-MS, in which the low background electrolyte concentration can be advantageous because competitive ionization is reduced.[13] Reversal of the direction of the plug migration has been achieved by simply reversing the direction of electric field wave. No notable band broadening was observed, but more thorough future studies will be performed to quantitate the effects of the reversal of plug direction on bandwidth.

The speed of migration is inherently slower in TWE than CE, because the electric field is alternating and consequently the velocity is slower than under an equivalent DC field set to maximum of the wave amplitude. Additionally, the ion trajectories are subject to both forward and reverse excursions as described previously.[10] In TWE, the velocity of the ions is dependent on the wavespeed.

Dispersion

Peak dispersion ultimately limits the peak width, making it an important factor in both the resolution and peak capacity of the separation. Currently, the peak widths and separation efficiencies achieved with CE are unparalleled and diffusion-limited peak widths can be achieved. Therefore, comparison of the bandwidth achieved in TWE with that of CE is an important criterion for evaluation of the performance of TWE. At the project outset, it was both hypothesized and hoped that TWE would provide reduced peak dispersion when compared with CE.

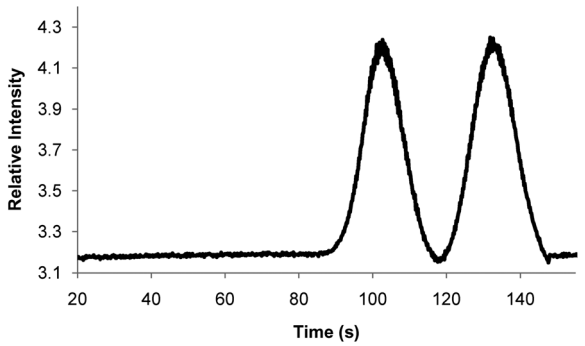

Fig. 5 Separation of a two dye mixture, 15 μM FL and 15 μM FLCA, at a frequency of 2 Hz, which is equivalent to a wavespeed of 160 mm s^{-1}.

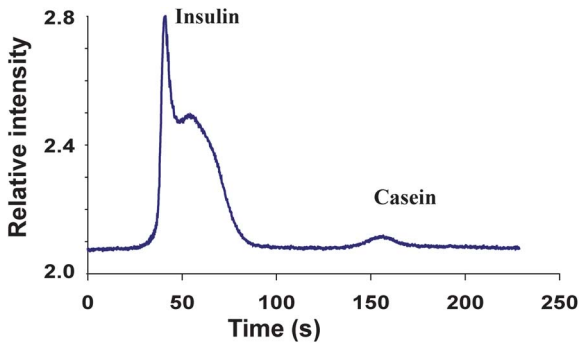

Fig. 6 Two proteins, insulin and casein, each labeled with FITC, are separated with a TWE device operating at a frequency of 2 Hz which is equivalent to a wavespeed of 160 mm s^{-1}.

The rationale is that in TWE the analytes are carried along the channel by a local electric field wave that traps the analyte molecules in potential wells at each electrode, suppressing longitudinal dispersion. Another way of conceptualizing the TWE process is that as the electrode potentials are altered, the molecules migrate toward the electrodes and are focused as they approach each electrode. To measure the dispersion, the peak width ($w_{1/2}$) of a fluorescein plug is measured at two locations in the microchannel that are separated by 8 mm for frequencies of one, two, and three Hz, as shown in Table 1 with the one Hz result highlighted in Fig. 4. As shown in Table 1, the velocity is dependent on the frequency and therefore the elution time of the peak decreases as the frequency is increased. For all three frequencies, the TWE peak width is less than the peak width for the corresponding times for the experimental stopped flow measurements and the theoretically predicted data. Theoretically, the peak area is independent of time and does not change with broadening. Experimentally, as the peak broadens a greater fraction of the sample is dispersed into regions where the concentration is below the LOD and therefore goes undetected, reducing the peak area as a function of time. During the stopped flow measurements, a lower magnification and NA objective was used to image the entire length of the band, resulting in higher (worse) LODs. Therefore, the peak widths observed in the stopped flow experimental data is are narrower than would be observed than if identical conditions to the TWE were used. These results demonstrate that high separation efficiencies and peak widths less than or equal to peak widths obtained with capillary electrophoresis at the diffusion limit can be achieved with TWE.

The measured dispersion values vary along the length of the TWE microchannel devices, with values up to about 30% greater in some devices. A probable cause for the variability of the dispersion values is variation in the microchannel height or other defects, resulting in variation in the electric field strength. Our modeling results indicate that the device is fairly sensitive to differences in height along the channel length. The model indicates that plug velocity varies by 10% for a ± 1 μm variation in channel height. These results indicate that the microchannel characteristics play a critical role in device performance.

Separation

In terms of system performance, a critical functionality is achieving separation of analytes and the quality of the separation. The ability to perform separations is clearly demonstrated through the separation of two dyes, fluorescein and FLCA, as shown in Fig. 5. The dyes are separated in a 30 mm long separation channel at 1-Hz and a resolution of 1.5 is achieved. The dyes have similar electrophoretic mobilities (FLCA: -3.04×10^{-4} cm^2 V^{-1} s; fluorescein: -2.86×10^{-4} cm^2 V^{-1} s) with the higher mobility FLCA eluting first as expected. A separation of the same dyes in CE yields a resolution of 2.8. A separation of the two standard proteins, insulin and casein, is shown in Fig. 6. As shown in Table 2, the reproducibility of the retention times and resolution is quite good, with RSDs for both values <1.5%. The assignments for the peaks were confirmed with separate injections and runs of the insulin and casein. Incomplete labeling of proteins is often problematic and can yield numerous protein species with heterogeneous labels. It is quite possible that the broad tail observed for the insulin peak in Fig. 6 is the result of heterogeneous labeling.

Sample enrichment with converging waves

Another exciting possibility in TWE-based devices is the enrichment of sample at the interface of two independent sets of electrode arrays. A device with two sets of electrode arrays arranged serially along the TWE channel was fabricated and the eight potentials were used to define two independently controlled electric field waves within the channel. Although the conditions for optimizing the enrichment are under investigation, initial results demonstrate that enrichment can be achieved in the microchannel by using converging electric field waves. As shown in Fig. 7, 40-fold enrichment is achieved when using 15 nM fluorescein as the initial sample concentration with this dual TWE array device. The narrow focused sample band has a $w_{1/2}$ of 107 ± 23 μm as shown in Table S1. In future experiments, the effect of the initial sample concentration will be investigated to determine if lowering the initial sample concentration will increase the maximum enrichment factor. It is notable that sample enrichment is achieved simply with two converging electric field waves without the need for buffer modification, incorporation of permselective materials, or flow balancing.

Table 2 Separation of FLCA and FL at 1.0 Hz

	FLCA			FL			
Replicate	Elution time (s)	$W_{1/2}$ (s)	Velocity (μm s^{-1})	Elution time (s)	$W_{1/2}$ (s)	Velocity (μm s^{-1})	Resolution
1	102.47	10.99	145.70	129.04	10.98	115.70	1.08
2	101.07	10.99	147.72	131.03	10.98	113.94	1.05
3	102.67	10.99	145.42	133.03	10.98	112.23	1.04
4	103.87	11.78	143.74	133.04	12.78	112.23	1.05
Average	102.52	11.18	145.64	131.53	11.43	113.52	1.06
SD	1.15	0.40	1.63	1.91	0.90	1.66	0.02
RSD(%)	**1.12**	**3.57**	**1.12**	**1.45**	**7.84**	**1.46**	**1.43**

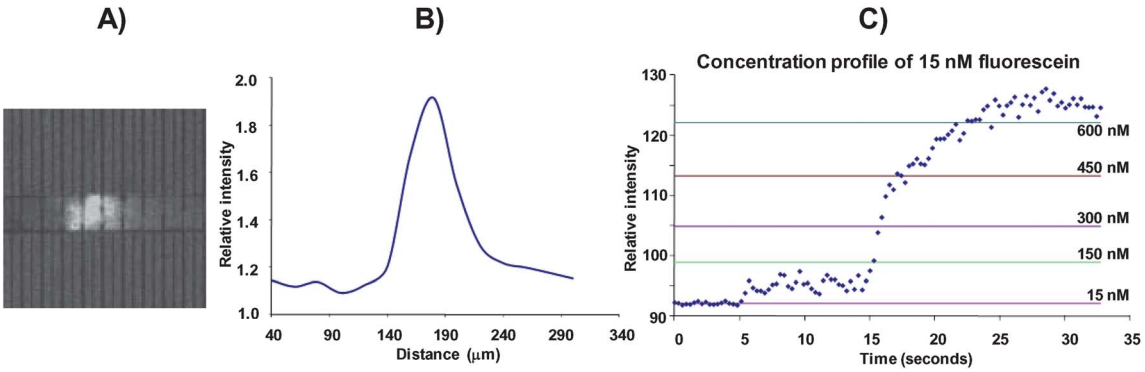

Fig. 7 Sample enrichment is achieved using a TWE device with two independently controlled sets of interdigitated electrode arrays with a total of eight applied potentials. The electric field waves of the two TWE arrays converge and both have wavespeeds of 2.0 Hz. A 15 nM fluorescein solution is injected continuously from the left side and an enrichment factor of >20 is achieved. In A), a fluorescent micrograph of the enriched band is shown; in B) the fluorescence intensity as a function of distance along the microchannel is shown, and in C) the fluorescence intensity as a function of time is shown with horizontal lines representing the intensity observed for the standards at the stated concentrations.

Conclusions

TWE is a promising new separation technique that can produce diffusion-limited peak widths in microfluidic separations similar to those achieved with CE. It should be noted that separation efficiencies achieved with microchannel electrophoresis are often much lower than those obtained with CE when capillaries and microchannels of the same material are used. An important contribution to increased band broadening in microchannels, when compared with capillaries, is the non-circular (and often trapezoidal) cross-section of the microchannel.[14] Additionally, TWE requires much lower voltages, on the order of $\pm$ 0.5 V, than CE, eliminating the high voltage requirement and improving portability of fieldable instruments. The lower voltages also fall below the potential of water hydrolysis, eliminating the bubbling problem that occurs in systems with higher voltage requirements. Having the electrodes within the microchannel, provides local control of the electric field that will provide advanced functionality, such as in-channel sample enrichment without buffer manipulation or integration of a permselective material. Sample enrichment can be easily achieved in the microchannel with two independently controlled electrode sets by having the two electric field waves converge at the junction of the two electrode sets. Injection of narrow sample bands is achieved with a pinched injection that can be driven either electrokinetically or hydrodynamically. The magnitude of the band broadening of the fluorescein band is less than or equal to the magnitude of the band broadening achievable with CE in the optimal diffusion-limited case for the three different wavespeeds of 1.0, 2.0, and 3.0 Hz. Separation of both model dyes and proteins is demonstrated. Future improvements in device design should improve the ease of fabrication and further reduce the band broadening. The experimental performance of the device reported herein suggests that TWE will be used in many future LOC applications for which it is well-suited.

Acknowledgements

This work is funded in part through NSF CBET-1066730 and the NSF RII award EPS0554328 for which the WV EPSCoR Office and the WVU Research Corporation provided matching funds.

References

1 J. M. Miller, *Chromatography: concepts and contrasts*, 2nd edn, John Wiley & Sons, New York, 2005.
2 J. W. Jorgenson and K. D. Lukacs, *Anal. Chem.*, 1981, **53**, 1298–1302.
3 J. W. Jorgenson and K. D. Lukacs, *Science*, 1983, **222**, 266–272.
4 M. T. Davis and T. D. Lee, *J. Am. Soc. Mass Spectrom.*, 1997, **8**, 1059–1069.
5 M. T. Davis, D. C. Stahl, S. A. Hefta and T. D. Lee, *Anal. Chem.*, 1995, **67**, 4549–4556.
6 D. Figeys, G. L. Corthals, B. Gallis, D. R. Goodlett, A. Ducret, M. A. Corson and R. Aebersold, *Anal. Chem.*, 1999, **71**, 2279–2287.
7 M. H. Lean, H. B. Hsieh and A. R. Volkel, 2005, 356–359.
8 M. H. Lean, A. R. Volkel, H. B. Hsieh, J.-P. Lu, J. H. Daniel, B. T. Preas and S. J. Limb, in *Proceedings of the 3rd Annual*

International IEEE EMBS Special Topic Conference on Microtechnologies in Medicine and Biology, Kahuku, Oahu, Hawaii, Editon edn.
9 H.-H. Wei, *Applied Physics Letters*, 2007, **90**, 204103/1–3.
10 B. F. Edwards, A. T. Timperman, R. L. Carroll, K. D. Jo, J. M. Mease and J. E. Schiffbauer, *Phys. Rev. Lett.*, 2009, **102**, 0761031–0761034.
11 Y. N. Xia and G. M. Whitesides, *Angew. Chem., Int. Ed.*, 1998, **37**, 551–575.
12 C. P. J. N. Lee and G. M. Whitesides, *Anal. Chem.*, 2003, **75**, 6544–6554.
13 J. H. Wahl, D. R. Goodlett, H. R. Udseth and R. D. Smith, *Electrophoresis*, 1993, **14**, 448–457.
14 S. Datta and S. Ghosal, *LOC*, 2009, **9**, 2537–2550.